New Journal of Physics
The open access journal at the forefront of physics

Deutsche Physikalische Gesellschaft DPG
IOP Institute of Physics

Published in partnership with: Deutsche Physikalische Gesellschaft and the Institute of Physics

OPEN ACCESS

RECEIVED
21 March 2016

REVISED
11 May 2016

ACCEPTED FOR PUBLICATION
19 May 2016

PUBLISHED
9 June 2016

PAPER

Electron spin relaxation can enhance the performance of a cryptochrome-based magnetic compass sensor

Daniel R Kattnig[1], **Jakub K Sowa**[1,4], **Ilia A Solov'yov**[2,3] **and P J Hore**[1]

[1] Department of Chemistry, University of Oxford, Physical and Theoretical Chemistry Laboratory, South Parks Road, Oxford OX1 3QZ, UK
[2] Department of Physics, Chemistry and Pharmacy, University of Southern Denmark, Campusvej 55, DK-5230 Odense M, Denmark
[3] On leave from A. F. Ioffe Physical Technical Institute, Politechnicheskaya Str. 26, 194021 St. Petersburg, Russia
[4] *Present address:* Department of Materials, University of Oxford, Parks Road, Oxford OX1 3PH, UK.

E-mail: peter.hore@chem.ox.ac.uk

Keywords: magnetoreception, quantum biology, migratory birds, animal navigation, radical pair mechanism

Supplementary material for this article is available online

Abstract

The radical pair model of the avian magnetoreceptor relies on long-lived electron spin coherence. Dephasing, resulting from interactions of the spins with their fluctuating environment, is generally assumed to degrade the sensitivity of this compass to the direction of the Earth's magnetic field. Here we argue that certain spin relaxation mechanisms can enhance its performance. We focus on the flavin–tryptophan radical pair in cryptochrome, currently the only candidate magnetoreceptor molecule. Correlation functions for fluctuations in the distance between the two radicals in *Arabidopsis thaliana* cryptochrome 1 were obtained from molecular dynamics (MD) simulations and used to calculate the spin relaxation caused by modulation of the exchange and dipolar interactions. We find that intermediate spin relaxation rates afford substantial enhancements in the sensitivity of the reaction yields to an Earth-strength magnetic field. Supported by calculations using toy radical pair models, we argue that these enhancements could be consistent with the molecular dynamics and magnetic interactions in avian cryptochromes.

1. Introduction

The rates and yields of free radical reactions are often sensitive to applied magnetic fields, a phenomenon known as the *radical pair mechanism* [1, 2]. It has been suggested [3] that migratory birds sense the direction of the Earth's magnetic field [4–7] by means of radical pairs formed photochemically in cryptochrome proteins located in their retinas [8]. Experimental and theoretical support for a radical pair mechanism of compass magnetoreception is accumulating (reviewed in [9–17]) although it is not yet clear whether cryptochrome is actually the sensor.

In vitro photo-excitation of the flavin adenine dinucleotide (FAD) cofactor in cryptochromes leads to the formation of radical pairs via sequential electron transfers along the 'Trp-triad', a chain of three tryptophan residues within the protein [18–21]. Donation of an electron to the excited singlet state of the FAD leads to the flavin radical, $FAD^{\bullet-}$, and the radical form of the terminal tryptophan, $TrpH_C^{\bullet+}$ (supplementary figure S1). This [$FAD^{\bullet-}$ $TrpH_C^{\bullet+}$] radical pair in both *Arabidopsis thaliana* cryptochrome-1 (*At*Cry1) and a closely related DNA photolyase has been shown to respond to weak magnetic fields (~1 mT) and has at least some of the properties required of a magnetic compass sensor [22, 23]. The origin of the magnetic field effect lies in a combination of the spin dynamics of the radical pair and its spin-selective recombination reactions, figures 1(a) and (b) and supplementary figure S1 [9].

Various spin interactions determine the magnetic field effect. The hyperfine interactions [24] of the electron spins with magnetic nuclei (mainly ^1H and ^{14}N) result in coherent, oscillatory interconversion of the electronic singlet and triplet states of the radical pair. The electronic Zeeman interaction with the external magnetic field

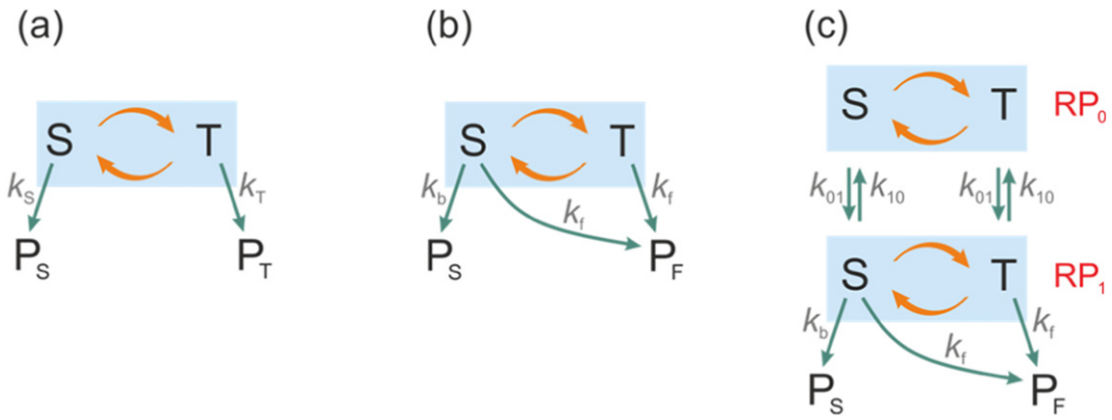

Figure 1. Radical pair reaction schemes. S and T are the singlet and triplet states of the radical pair. The curved orange arrows indicate the coherent interconversion of the S and T states by hyperfine and Zeeman interactions. k_S, k_T, k_b, and k_f are rate constants. The electron Zeeman interaction alters the extent and timing of S $\leftrightarrow$ T interconversion in the radical pair so that the final yields of the reaction products, once all the radicals have reacted, depend on the orientation of the radical pair with respect to the magnetic field. (a) A generic radical pair reaction scheme in which the S and T states are able to react spin-selectively to form singlet and triplet products, P_S and P_T, respectively. (b) A reaction scheme for [$FAD^{\bullet-}$ $TrpH_C^{\bullet+}$] (RP_1) in *At*Cry1 in which triplet recombination cannot occur. Instead, the S and T states undergo a non-spin-selective reaction (protonation of $FAD^{\bullet-}$, deprotonation of $TrpH_C^{\bullet+}$, or both) with the same rate constant to form a product P_F. (c) An extension of (b) in which RP_0 ([$FAD^{\bullet-}$ $TrpH_B^{\bullet+}$]) is formed reversibly by electron hopping ($TrpH_B$ $TrpH_C^{\bullet+}$ $\rightleftarrows$ $TrpH_B^{\bullet+}$ $TrpH_C$) during the lifetime of RP_1. In both (b) and (c), the singlet product, P_S, is the ground state of the protein.

modifies this time-dependence, altering the probability of spin-dependent radical recombination and changing the yields of the reaction products (figures 1(a) and (b)). The anisotropy of the hyperfine interactions causes the effect of the external field to depend on its direction, as required for a compass sensor. Two other important interactions—usually neglected in this context—are the electron–electron exchange and dipolar couplings [25, 26], both of which depend on r, the distance between the centres of electron spin density in the two radicals. The exchange interaction is usually assumed to have the exponential form:

$$J(r) = J_0 \exp(-\beta r), \tag{1}$$

with a range parameter $\beta = 14\ \mathrm{nm}^{-1}$ for radicals embedded in a protein [25, 27]. The strength of the interaction, J_0, has a complex dependence on the electronic properties of the radicals and is difficult to calculate with any accuracy. The dipolar interaction, however, can reliably be obtained by assuming the electron spins to be point dipoles (normally an excellent approximation for radical pairs [25]):

$$D(r) = -\frac{2.785\ \mathrm{mT}}{(r/\mathrm{nm})^3} = -\frac{77.80\ \mathrm{MHz}}{(r/\mathrm{nm})^3}. \tag{2}$$

In the absence of other spin interactions, $J(r)$ and $D(r)$ remove the degeneracy of the singlet (S) and the three triplet (T_{+1}, T_0, T_{-1}) states:

$$E(\mathrm{S}) = +J(r), \quad E(\mathrm{T}_m) = -J(r) + D(r)\left(m^2 - \frac{2}{3}\right); \tag{3}$$

(m, the magnetic quantum number of the triplet, equals 0 or ± 1). These interactions hinder efficient singlet–triplet interconversion and so degrade the sensitivity of the radical pair to the geomagnetic field [25].

The magnetically sensitive [$FAD^{\bullet-}$ $TrpH_C^{\bullet+}$] radical pair in *At*Cry1 [23] has $r = 1.90$ nm [28], giving $D(r) = -11$ MHz and $|J(r)| = 6.3$ MHz (assuming $|J_0| \approx 8.0 \times 10^7$ T and $\beta = 14\ \mathrm{nm}^{-1}$ [25]). Experimental measurements of $J(r)$ for [$FAD^{\bullet-}$ $TrpH_C^{\bullet+}$] in two DASH-type cryptochromes are in rough agreement with this estimate: +2.0 MHz for *Xenopus laevis* [29] and +4.2 MHz for *Synechocystis* [30]. A more exact calculation of $D(r)$, avoiding the point-dipole approximation, confirmed the −11 MHz value to within 0.6 MHz [25]. It is therefore clear that both $|J(r)|$ and $|D(r)|$ are likely to be larger than the electron Zeeman interaction (~1.4 MHz) with the Earth's magnetic field (~50 μT), and cannot therefore be dismissed.

Although values of $|J(r)|$ or $|D(r)|$ larger than a few MHz would be sufficient to mar the performance of a radical pair as a geomagnetic sensor, the effects of the two interactions can partially cancel under certain circumstances, specifically when $D(r)/J(r) \approx +6$ or -3 [25]. Using estimates of $|J_0|$ derived from data on photosynthetic reaction centre proteins [31–33], it has been argued that such ratios can be expected when $r \approx 2.0 \pm 0.2$ nm, i.e. a separation close to that of $FAD^{\bullet-}$ and $TrpH_C^{\bullet+}$ in cryptochromes (~1.9 nm) [25]. However, the values of $J(r)$ and $D(r)$ are not known for any of the four avian cryptochromes, and it has not been established how effective the cancellation would be for radicals as complex as flavin and tryptophan. It is

therefore appropriate to ask whether the damaging effects of $J(r)$ and $D(r)$ could be circumvented in some other way. One possibility, discussed later, is that 'the quantum Zeno effect immunises the avian compass against the deleterious effects of exchange and dipolar interactions' [34]. Here, we examine whether electron spin relaxation could come to the rescue.

Spin relaxation, the process that drives the electron–nuclear spin system of the radical pair towards thermal equilibrium [24], is normally expected to attenuate the sensitivity of the compass by destroying the spin coherence that is essential for its operation [35]. It seems plausible that the optimum performance would require negligible loss of coherence during the lifetime of the radical pair. There have been several theoretical treatments of spin relaxation in the context of magnetoreception, almost all of which have dealt with generic relaxation mechanisms furnished with phenomenological rate constants [36–41]. Intriguingly, a few of these studies have indicated that the compass sensitivity could be *enhanced* by the inclusion of certain abstract spin relaxation pathways [37, 38, 40, 42, 43]. In the following, we discuss the spin relaxation that arises from realistic spin interactions modulated by realistic protein dynamics. Specifically, we show that the time dependence of $J(r)$ and $D(r)$ arising from stochastic fluctuations in the separation of the $FAD^{\bullet-}$ and $TrpH_C^{\bullet+}$ radicals in cryptochrome has the potential to boost the magnetic field effect and so counteract the detrimental effects these interactions would have in the absence of molecular motion.

2. *J*-modulation by fluctuations in *r*

We start by establishing the principle that the harmful effect of an exchange interaction on a radical pair compass can be alleviated by fluctuations in the strength of that interaction. To do so, we chose the simplest possible radical pair comprising two electron spins, one of which is coupled to a single spin-$\frac{1}{2}$ nucleus via an anisotropic hyperfine interaction. The eigenvalues of the anisotropic hyperfine tensor [24], $A_{xx} = A_{yy} = 0$, $A_{zz} = 42$ MHz, were chosen to resemble the hyperfine tensor of the N5 interaction in $FAD^{\bullet-}$ [44]. Singlet and triplet pairs were allowed to react to form distinct products (figure 1(a)) with identical rate constants, $k = k_S = k_T = 10^6\ s^{-1}$, such that the radical pair lifetime was 1 μs. At time $t = 0$, the radical pair was in a pure singlet state with no nuclear polarisation. The performance of this toy compass was judged by the anisotropy of the singlet yield:

$$\Delta\Phi_S = \Phi_S(0) - \Phi_S(90^\circ), \tag{4}$$

where $\Phi_S(\theta)$ is the final yield of the singlet product (P_S in figure 1(a)) and θ is the angle between the external magnetic field (50 μT) and the symmetry axis of the hyperfine tensor.

$\Phi_S(\theta)$ was determined using the equation of motion for the radical pair density operator, $\hat{\rho}(t)$:

$$\frac{d\hat{\rho}(t)}{dt} = -i[\hat{H}_0, \hat{\rho}(t)] - k\hat{\rho}(t) - k_{STD}(\hat{P}^S\hat{\rho}(t)\hat{P}^T + \hat{P}^T\hat{\rho}(t)\hat{P}^S) = -\hat{\hat{\Omega}}\hat{\rho}(t). \tag{5}$$

$\hat{H}_0$ is the time-independent part of the spin Hamiltonian:

$$\hat{H}_0 = \gamma_e B_0[(\hat{S}_{Ax} + \hat{S}_{Bx})\sin\theta + (\hat{S}_{Az} + \hat{S}_{Bz})\cos\theta] + A_{zz}\hat{S}_{Az}\hat{I}_z - J_{av}\left(2\hat{\boldsymbol{S}}_A \cdot \hat{\boldsymbol{S}}_B + \frac{1}{2}\hat{E}\right), \tag{6}$$

in which the three terms are, respectively, the electron Zeeman, electron–nuclear hyperfine, and average exchange interactions. $\hat{\boldsymbol{S}}_A$ and $\hat{\boldsymbol{S}}_B$ are the electron spin angular momentum operators of the two radicals, and $\hat{\boldsymbol{I}}$ is the spin operator of the nucleus in radical A. $B_0 = 50$ μT is the strength of the external magnetic field. The other terms in equation (5) account for the radical recombination reactions and the effects of fluctuations in $J(r)$. The latter is derived in appendix A. k_{STD} is the rate constant of the spin relaxation caused by J-modulation, and $\hat{P}^S$ and $\hat{P}^T$ are the singlet and triplet projection operators. If the fluctuations in the exchange interaction occur on a faster timescale than the coherent spin dynamics, k_{STD} is given by (appendix A)

$$k_{STD} = 4\langle[J(r(t)) - J_{av}]^2\rangle\tau_c, \tag{7}$$

where $\langle\cdots\rangle$ indicates a time average, $J_{av} = \langle J(r(t))\rangle$, and the correlation time τ_c characterises the timescale of the fluctuations in r. The rate of relaxation is thus proportional to the mean square deviation of the exchange parameter from its mean value and is faster the slower the fluctuations. It is clear from equation (5) that J-modulation relaxes density matrix elements of the type $\langle S|\ \hat{\rho}(t)|T_m\rangle$; it is therefore referred to as a 'singlet–triplet dephasing' (STD) mechanism [45]. We note that the relaxation term in equation (5) can also be obtained phenomenologically using Lindblad noise operators, $\hat{L}_j$ [36, 46]:

$$\frac{d\hat{\rho}(t)}{dt} + i[\hat{H}_0, \hat{\rho}(t)] + k\hat{\rho}(t) = k_{STD}\sum_j\left[\hat{L}_j\hat{\rho}(t)\hat{L}_j^\dagger - \frac{1}{2}(\hat{L}_j^\dagger\hat{L}_j\hat{\rho}(t) + \hat{\rho}(t)\hat{L}_j^\dagger\hat{L}_j)\right] \tag{8}$$

with $\hat{L}_j = \{\hat{P}^S, \hat{P}^T\}$ or $2^{-1/2}(\hat{P}^S - \hat{P}^T)$.

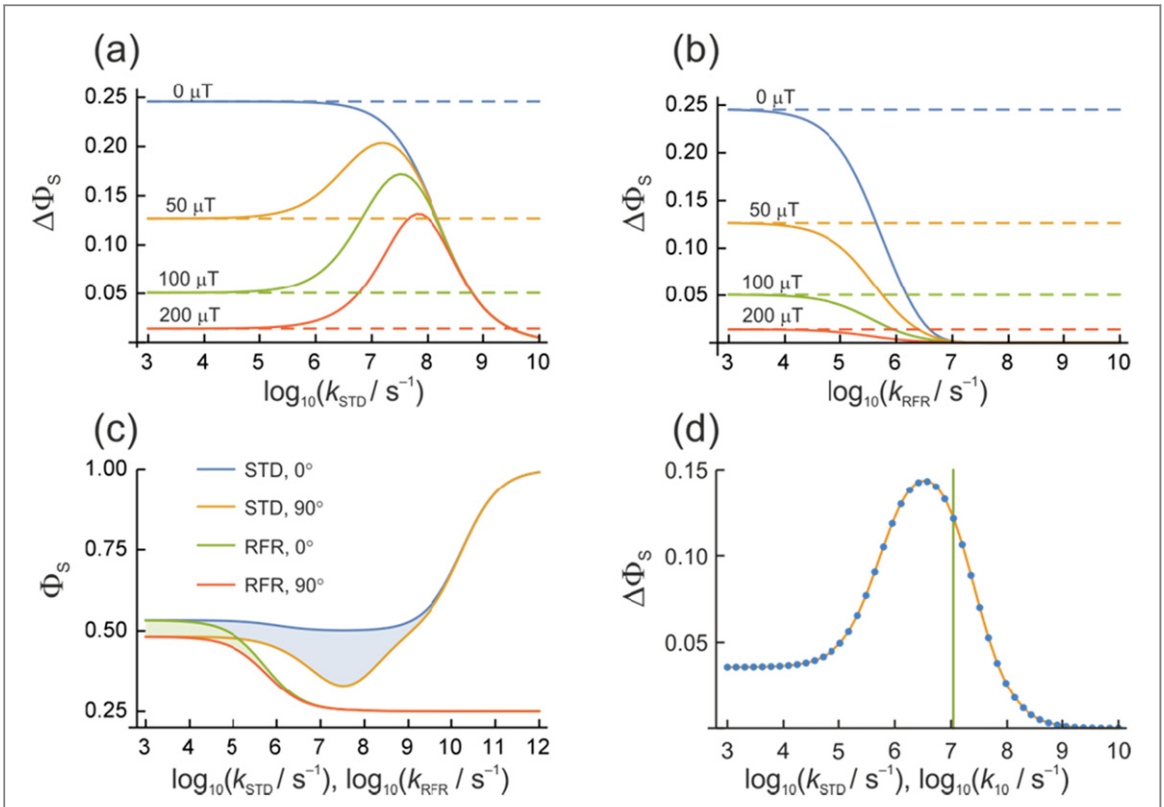

Figure 2. Anisotropy of the singlet yield ($\Delta\Phi_S$) of a toy radical pair as a function of the spin relaxation rate constant. The solid lines in (a) and (b) show $\Delta\Phi_S$ (equation (4)) for the STD and RFR mechanisms, respectively, for four values of J_{av}. The dashed lines are $\Delta\Phi_S$ in the absence of spin relaxation. (c) The singlet yield, $\Phi_S(\theta)$, when the magnetic field is parallel ($\theta = 0$) and perpendicular ($\theta = 90°$) to the symmetry axis of the hyperfine interaction, for the STD and RFR mechanisms with $J_{av} = 100\ \mu$T. (d) $\Delta\Phi_S$ for the STD relaxation mechanism induced by electron hopping. Blue dots: $\Delta\Phi_S(k_{10})$ calculated with explicit two-site electron hopping; orange line: $\Delta\Phi_S(k_{STD})$ calculated using equation (9). The green line indicates the value of k_{10} ($1.1 \times 10^7\ s^{-1}$) determined from experiments on *At*Cry1 [23]. (a)–(c) $D = 0$, magnetic field $= 50\ \mu$T, principal components of the hyperfine interaction, $(A_{xx}, A_{yy}, A_{zz}) = (0.0, 0.0, +1.5)$ mT, recombination rate constants $= k_S = k_T = 10^6\ s^{-1}$ (figure 1(a)). (d) As for (a)–(c), with $J(RP_0) = 800$ mT, $J(RP)_1 = 0.1$ mT, $k_{01} = 1.0 \times 10^{10}\ s^{-1}$, $k_b = 4.9 \times 10^5\ s^{-1}$, $k_f = 2.5 \times 10^5\ s^{-1}$ (see figure 1(b) for definitions of the rate constants).

Finally, the singlet yield once all radicals have recombined is:

$$\Phi_S(\theta) = k\int_0^\infty \mathrm{Tr}[\hat{P}^S\hat{\rho}(t)]\,\mathrm{d}t = k\int_0^\infty \mathrm{Tr}[\hat{P}^S \exp(-\hat{\hat{\Omega}}t)\hat{\rho}(0)]\,\mathrm{d}t, \tag{9}$$

where the superoperator $\hat{\hat{\Omega}}$ is defined in equation (5) and $\hat{\rho}(0) = \frac{1}{2}\hat{P}^S$.

Figure 2(a) plots the anisotropy $\Delta\Phi_S$ (equation (4)) versus k_{STD} for four values of J_{av}. When k_{STD} is small (e.g. $10^3\ s^{-1}$), there is essentially no relaxation during the 1 μs lifetime of the radicals. In this limit, $\Delta\Phi_S$ is dramatically reduced when the average exchange interaction is comparable to or stronger than the geomagnetic field (50 μT). However, when $J_{av} \neq 0$, values of k_{STD} greater than $\sim 10^6\ s^{-1}$ cause $\Delta\Phi_S$ to rise towards the values appropriate for $J_{av} = 0$. When the relaxation is faster still ($k_{STD} > 10^8\ s^{-1}$), $\Delta\Phi_S$ drops towards zero. Fluctuations in $J(r)$ resulting in intermediate relaxation rates ($10^6\ s^{-1} < k_{STD} < 10^8\ s^{-1}$) therefore boost the compass sensitivity well above the level expected for a time-independent exchange interaction (dashed lines in figure 2(a)). Similar behaviour was found for modulation of the dipolar interaction (appendix B and supplementary figure S2) and for the reaction scheme in figure 1(b) (supplementary figure S3).

To put figure 2(a) in context, J-modulation was compared with a 'random fields' relaxation (RFR) mechanism in which unspecified, uncorrelated molecular motions cause the expectation values of all three spin angular momentum operators ($\hat{S}_x$, $\hat{S}_y$, and $\hat{S}_z$) of both electrons to relax independently with the same rate constant, k_{RFR} (appendix C). As shown in figure 2(b), this relaxation mechanism does not enhance $\Delta\Phi_S$ but causes it to fall towards zero at much smaller values of the rate constant than was the case in figure 2(a). Clearly, not all relaxation mechanisms are able to rescue the sensitivity of a radical pair compass.

To shed light on the differences between figures 2(a) and (b), figure 2(c) plots $\Phi_S(\theta)$ for $\theta = 0$ and $\theta = 90°$ as a function of the relaxation rate constant for the two mechanisms (with $J_{av} = 100\ \mu$T). It can be seen that very fast relaxation ($>10^{10}\ s^{-1}$) destroys the anisotropy either by locking the radical pair into its initial singlet state (STD) or by relaxing the spins to the equilibrium state in which the singlet probability is 0.25 (RFR). For rate constants between $10^6\ s^{-1}$ and $10^8\ s^{-1}$, STD is much less effective at relaxing $\Phi_S(\theta)$ towards 0.25 when the

magnetic field is parallel to the hyperfine axis ($\theta = 0$) than when it is perpendicular ($\theta = 90°$). For the STD mechanism, therefore, the anisotropy in the reaction yield is considerably larger when $10^6\ s^{-1} \lesssim k_{STD} \lesssim 10^8\ s^{-1}$ than in the absence of relaxation ($k_{STD} < 10^4\ s^{-1}$). The RFR mechanism, by contrast, relaxes the spins isotropically and so drives $\Delta\Phi_S$ monotonically to zero as k_{RFR} is increased.

3. *J*-modulation by electron hopping

STD has been invoked to account for the observed magnetic-field dependence of the flavin–tryptophan radical pair reaction in *At*Cry1 [23]. *J*-modulation was considered to arise from reversible electron hopping between the distal and medial members of the Trp-triad, i.e. [$FAD^{\bullet-}$ $TrpH_B$ $TrpH_C{}^{\bullet+}$] ⇄ [$FAD^{\bullet-}$ $TrpH_B{}^{\bullet+}$ $TrpH_C$] (figure 1(c)). As described above, the former (denoted RP_1) has $r_1 = 1.90$ nm and exchange and dipolar interactions of a few MHz; the latter (denoted RP_0) has a centre-to-centre distance $r_0 = 1.32$ nm in *At*Cry1 and estimated interactions: $|J(r_0)| \approx 21$ GHz, $D(r_0) = -34$ MHz [25]. With such a large exchange interaction in RP_0, reversible electron hopping results in strong modulation of $J(r)$ and potentially rapid relaxation of singlet–triplet coherences in RP_1. Provided k_{01}, the electron hopping rate constant for $RP_0 \rightarrow RP_1$, is not much larger than $|J(r_0)|$, then every time RP_1 is converted into RP_0 the coherence experiences a large phase shift before the electron jumps back. Under these conditions, the dephasing rate constant k_{STD} in equation (5) is expected to be equal to k_{10}, the rate constant for $RP_0 \leftarrow RP_1$ [23].

This prediction can be verified with a toy model similar to that used above. Figure 2(d) shows the singlet yield anisotropy determined (i) as a function of k_{STD} using equation (5) and (ii) as a function of k_{10} by solving a Liouville equation containing explicit reversible electron hopping between RP_0 and RP_1, coherent spin dynamics in both radical pairs, and spin-selective recombination for RP_1 (figure 1(c) and appendix D). The parameters for method (ii) were chosen to approximate those determined from the observed magnetic field effects on [$FAD^{\bullet-}$ $TrpH_C{}^{\bullet+}$] in *At*Cry1 [23]. The two calculations are in excellent agreement confirming that the dephasing rate constant is indeed given by k_{10}. Note also that the value of k_{10} ($= 1.1 \times 10^7\ s^{-1}$) determined from the magnetic field effects on *At*Cry1 [23] corresponds to a position in figure 2(d) close to the maximum enhancement of $\Delta\Phi_S$. However, this should be treated with caution because of our use of a grossly simplified spin system for figure 2(d) (one nuclear spin instead of ~10; eight spin states instead of $\sim 2^{12}$).

4. *J*-modulation in cryptochrome

We now turn to STD spin relaxation for the [$FAD^{\bullet-}$ $TrpH_C{}^{\bullet+}$] radical pair in cryptochrome. Fluctuations in the separation and relative orientation of the two radicals were characterised by means of all-atom molecular dynamics (MD) simulations [47]. The calculations were performed using a modified version of the crystal structure of *At*Cry1 (PDB ID 1U3C [28]) containing the flavin radical, $FAD^{\bullet-}$, and the radical form of the terminal residue of the Trp-triad, $TrpH_C{}^{\bullet+}$ (W324) with force-field parameters and atomic charges as in [48]. The protein was solvated in an aqueous solution of 50 mM NaCl in a periodic box of dimensions $103 \times 111 \times 99\ Å^3$ containing a total of 113 455 atoms. After extensive equilibration, seven statistically independent MD trajectories, three spanning 300 ns and four covering 100 ns, were accumulated for the microcanonical ensemble at 300 K. The initial configuration of the system was identical in the seven simulations; stochastic behaviour emerged from the Langevin thermostat [49], as implemented in NAMD [50]. The protein dynamics were sampled at intervals of 0.5 or 5 ps. The accumulated trajectories cover 1.3 μs. Because the motions of the radicals are considerably faster than both spin relaxation and radical recombination, it is not necessary for the simulations to include the reactions or to span the lifetime of the radicals. Electron hopping between $TrpH_B$ and $TrpH_C$ [23] was not included. Further details of the simulations can be found in [47].

Motional correlation functions, calculated from the MD trajectories, were used to obtain spectral densities and hence a Redfield relaxation superoperator [51, 52] which, when combined with (i) electron Zeeman and hyperfine interactions, (ii) average exchange and dipolar interactions, and (iii) spin-selective recombination reactions, allowed calculation of the singlet yield $\Phi_S(\theta, \phi)$, where the polar angles θ and ϕ specify the direction of the external 50 μT magnetic field (appendix A, equation (20)). The slow relaxation arising from cross-correlation of the exchange and the dipolar interactions was neglected. The reaction yield anisotropy, $\Delta\Phi_S$, was calculated as the difference between the maximum and minimum values of $\Phi_S(\theta, \phi)$. Spin relaxation induced by fluctuations in the hyperfine interactions was the subject of [47] and is not treated here. The forward electron transfer steps along the Trp-triad are complete within a nanosecond which is too fast for singlet–triplet coherence to be generated in the intermediate radical pairs [$FAD^{\bullet-}$ $TrpH_A{}^{\bullet+}$] and [$FAD^{\bullet-}$ $TrpH_B{}^{\bullet+}$]. Consequently, STD relaxation is expected to occur only in [$FAD^{\bullet-}$ $TrpH_C{}^{\bullet+}$].

Figures 3(a)–(c) show the variation in r, $J(r)$ and $D(r)$ over the course of MD trajectories spanning 1.3 μs in total. $J(r)$ and $D(r)$ were calculated using equations (1) and (2), with $|J_0| = 8 \times 10^7$ T and $\beta = 14\ nm^{-1}$. The

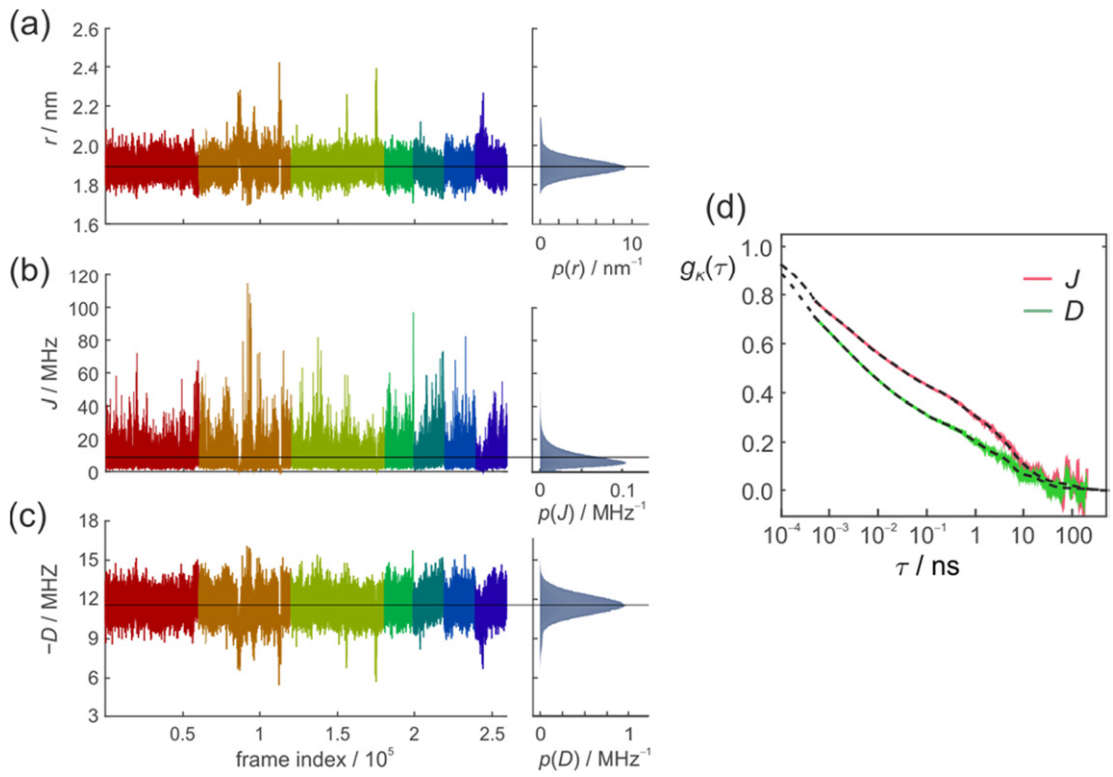

Figure 3. Variation in (a) the radical separation, (b) the exchange interaction and (c) the dipolar interaction of [$FAD^{\bullet-}$ $TrpH_C^{\bullet+}$] in *At*Cry1. The MD trajectories were sampled every 5 ps. The different colours indicate different MD runs starting from the same configuration. The horizontal lines in the three panels give the mean values: r_{av}, J_{av}, and D_{av}. Shown on the right-hand side of (a)–(c) are the corresponding distribution functions. (d) Auto-correlation functions, $g_K(\tau)$ (equation (10)), for the exchange (pink) and dipolar (green) interactions in [$FAD^{\bullet-}$ $TrpH^{\bullet+}$] in *At*Cry1, calculated from the MD trajectories. The dashed black lines are the multi-exponential fits used to calculate the relaxation superoperator; both have been extrapolated back to $\tau = 100$ fs. $g_r(\tau)$ decays to ~0.79 within the first 500 fs; motions on this timescale are far too fast to cause spin relaxation.

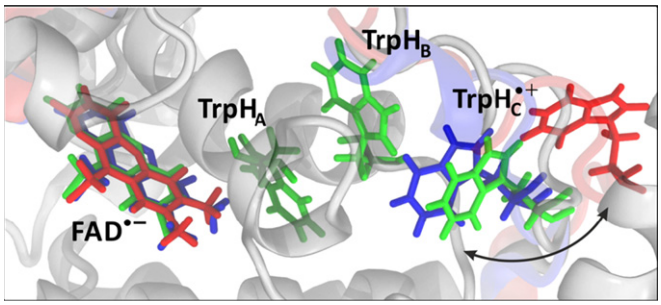

Figure 4. Molecular dynamics structures of *At*Cry1 in the region of the FAD and Trp triad. The positions of the two components of the radical pair ($FAD^{\bullet-}$ and $TrpH_C^{\bullet+}$), the proximal and medial tryptophans ($TrpH_A$ and $TrpH_B$), and the backbone in the average structure ($r_{av} = 1.89$ nm) are shown in green and grey. The positions of the two radicals, and the backbone in the region of $TrpH_C^{\bullet+}$, are shown in red and blue for the structures with, respectively, the largest ($r_{max} = 2.43$ nm) and smallest ($r_{min} = 1.69$ nm) radical separations. The curved arrow indicates the range of motion of $TrpH_C^{\bullet+}$.

mean distance between the centres of spin density (± standard deviation; see supplementary figure S4) is $r_{av} = 1.89 \pm 0.05$ nm. The mean interaction strengths (± standard deviation) are $|J_{av}| = 8.42 \pm 5.64$ MHz and $D_{av} = -11.5 \pm 0.9$ MHz. The maximum and minimum separations are $r_{max} = 2.43$ nm and $r_{min} = 1.69$ nm, so that $|J(r_{min})| = 115$ MHz, $|J(r_{max})| = 3.85$ kHz, $D(r_{min}) = -16.1$ MHz, and $D(r_{max}) = -5.5$ MHz.

Figure 4 gives an impression of the positions of the two radicals in *At*Cry1 in the average structure and in the two extreme conformations, $r = r_{min}$ and $r = r_{max}$. The variation in the radical separation is mainly attributable to the greater mobility of the $TrpH_C^{\bullet+}$ radical compared to the more snugly bound $FAD^{\bullet-}$ radical located in the centre of the protein. Representations of the semi-occupied molecular orbitals and the spin densities in the two radicals are shown in supplementary figure S4.

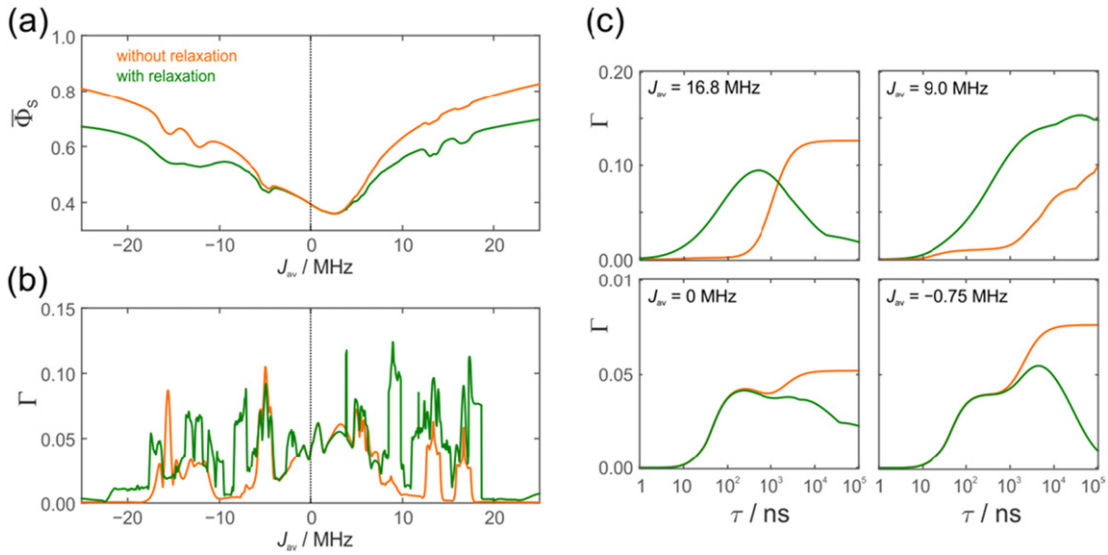

Figure 5. Dependence of (a) the average singlet yield ($\bar{\Phi}_S$) and (b) the fractional anisotropy of the singlet yield ($\Gamma = \Delta\Phi_S/\bar{\Phi}_S$) on the mean exchange interaction, J_{av}. (c) Dependence of Γ on the radical pair lifetime for selected values of J_{av}. The green and orange lines are for radical pairs respectively with and without the spin relaxation caused by fluctuations in the exchange and dipolar interactions. For all three panels, the magnetic field was 50 μT. In (a) and (b) the radical pair lifetime was $\tau = k_S^{-1} = k_T^{-1} = 1$ μs. [$FAD^{\bullet-}$ $TrpH_C^{\bullet+}$] was modelled by including the N5 and N10 hyperfine interactions of $FAD^{\bullet-}$ in one radical and no hyperfine interactions in the other radical (i.e. a total of 36 spin states). The hyperfine and average electron–electron dipolar interaction tensors are given in the supporting information of [47]. The relaxation effects in the lower two panels in (c) arise entirely (left) and mostly (right) from *D*-modulation.

Given the uncertainty in the value of J_0 (equation (1)), we henceforth treat $|J_{av}|$ as an adjustable parameter and model the exchange interaction as $J(r) = J_{av}\exp(-\beta(r - r_{av}))$, with $\beta = 14$ nm^{-1} and $r_{av} = 1.89$ nm as above. Except for very small values of $|J_{av}|$, the fluctuations in $J(r)$ are much larger than those in $D(r)$, meaning that *J*-modulation should be the dominant source of spin relaxation.

The auto-correlation functions

$$g_K(\tau) = \langle [K(t) - K_{av}][K(t+\tau) - K_{av}] \rangle \tag{10}$$

($K = r, J$, or D, and $K_{av} = \langle K(t) \rangle$) that characterise the relevant motions of the radical pair are highly non-exponential as a result of motions on timescales ranging from picoseconds to nanoseconds (figure 3(d)). The average time constant for the decay of $g_r(\tau)$ (8.5 ns) is determined mainly by low-amplitude components in the range $\tau \geqslant 10$ ns. In combination with the large fluctuations in $J(r(t))$ noted above, these comparatively slow motions tend to dominate the spin relaxation. By contrast, the rapidly decaying components of $g_r(\tau)$ ($\tau < 500$ fs) are of minor importance. The average time constants for $g_J(\tau)$ and $g_D(\tau)$ are 8.5 ns and 7.6 ns, respectively, reflecting the different *r*-dependence of the two interactions.

Figures 5(a) and (b) show, respectively, the singlet yield averaged over all directions of the magnetic field, $\bar{\Phi}_S$, and the relative anisotropy, $\Gamma = \Delta\Phi_S/\bar{\Phi}_S$, both as functions of J_{av}. The lifetime of the radical pair ($\tau = k_S^{-1} = k_T^{-1}$) was 1 μs. When $|J_{av}| < 5$ MHz, the protein dynamics have a minimal effect on $\bar{\Phi}_S$ (figure 5(a)). For larger $|J_{av}|$, relaxation tends to reduce $\bar{\Phi}_S$ towards the statistical value of 0.25. The effect of spin relaxation on the anisotropy (figure 5(b)) is small when $|J_{av}|$ is outside the range 2 MHz $< |J_{av}| <$ 25 MHz but shows a complex behaviour within this range. For most of these intermediate values of $|J_{av}|$, STD boosts the anisotropy above that found when relaxation is excluded. Γ is particularly strongly enhanced for positive values of the exchange interaction (7 MHz $< J_{av} <$ 18 MHz).

Figure 5(c) offers additional insight by plotting the relative singlet yield anisotropy Γ against the radical pair lifetime for a few representative values of J_{av}. In the absence of relaxation (orange lines), Γ is small for very short lifetimes ($\tau < 10$ ns), grows as τ approaches the reciprocal of the Larmor period (~700 ns), and eventually reaches a plateau when $\tau > \sim 10$ μs. When relaxation is included (green lines) and $|J_{av}|$ is small (e.g. 0.0 and −0.75 MHz), the anisotropy is always less than or equal to that in the absence of relaxation. For larger J_{av} however (e.g. +16.8 MHz and +9.0 MHz), the relaxation causes a substantial increase in Γ for radical pairs with intermediate lifetimes (10 ns $< \tau <$ 1 μs). For example, when $J_{av} = +16.8$ MHz, and $\tau = 100$ ns, the STD mechanism boosts Γ by a factor of 34. No enhancement of any magnitude was found in our earlier study of the relaxation resulting from fluctuations in the hyperfine interactions in $FAD^{\bullet-}$ and $TrpH_C^{\bullet+}$ [47].

In summary, unless the mean exchange interaction is too large or too small, the thermal fluctuations in the separation of the $FAD^{\bullet-}$ and $TrpH_C^{\bullet+}$ radicals in cryptochrome can induce spin relaxation of such a rate as to enhance the magnetic sensitivity, sometimes quite substantially.

5. Discussion

In the following paragraphs we discuss other ways in which Nature might have avoided the problems posed by exchange and dipolar interactions in a [$FAD^{\bullet-}$ $TrpH_C^{\bullet+}$] cryptochrome magnetosensor. We then comment on possible reasons why the sensitivity enhancements afforded by fluctuations in the radical separation might not be manifested in cryptochrome.

5.1. Asymmetric recombination rates

Dellis and Kominis have suggested that harmful effects of exchange and dipolar interactions may be avoided if the radical recombination kinetics are highly asymmetric [34]. They argued that the anisotropy $\Delta\Phi_S$ can be larger when the rate constants for recombination of the singlet and triplet states (figure 1(a)) are such that $k_T \gg k_S$ rather than $k_T = k_S$. We believe this is unlikely to occur in a cryptochrome magnetoreceptor, for two reasons. First, our experience with toy models (supplementary figure S5) suggests that any benefit arising from the condition $k_T \gg k_S$ only accrues when the average exchange and/or dipolar interactions are stronger than the effective hyperfine interactions in both radicals, viz. 39 MHz $\equiv$ 1.40 mT for $FAD^{\bullet-}$ and 54 MHz $\equiv$ 1.94 mT for $TrpH_C^{\bullet+}$ [23]. A value of $|J_{av}|$ in excess of 40–50 MHz would result in such a small singlet yield anisotropy (see, e.g., figure 5(b)) that it would probably be beyond rescue by even the most favourable kinetics [53]. Second, a reaction scheme in which singlet and triplet radical pair states both recombine spin selectively to give distinct products (figure 1(a)) is not appropriate for [$FAD^{\bullet-}$ $TrpH_C^{\bullet+}$] because there is no energetically accessible molecular triplet state in cryptochrome to which the triplet radical pair could recombine [23]. Rather, one should consider a scheme (figure 1(b)) in which the singlet recombines spin selectively (to form the ground state of the protein, with rate constant k_b) in competition with a reaction such as (de)protonation of one or both of the radicals [23] whose rate constant (k_f) is independent of the spin state of the pair. For such a reaction scheme, there is no advantage to be gained from highly asymmetric rate constants (supplementary figure S5).

5.2. Alternative radical pairs

Despite the finding that [$FAD^{\bullet-}$ $TrpH_C^{\bullet+}$] in isolated *At*Cry1 *in vitro* responds to relatively weak magnetic fields [23], it is not clear that this radical pair would necessarily be the sensor in an *in vivo* cryptochrome magnetoreceptor. Protein–protein and protein–ligand interactions in a cellular environment could result in a different, and possibly more sensitive, radical pair via an alternative or extended electron transfer pathway [44, 54, 55]. It is therefore important to ask whether Nature could have contrived a cryptochrome-based magnetic sensor in which the exchange and dipolar interactions are so weak that they do not adversely affect its performance. This is a complex question with no clear answer. Using equation (1) with $\beta = 14\ \mathrm{nm}^{-1}$, an increase in r of only 0.33 nm would result in a 100-fold reduction in $J(r)$, making it negligibly small. This might be achieved if a fourth tryptophan residue were involved in the electron transfer chain that creates the magnetically sensitive radical pair [56, 57]. However such an increase in the separation of the radicals would also slow down the reverse electron transfer reaction by about two orders of magnitude, prolong the lifetime of the radical pair and make it much more vulnerable to loss of coherence by spin relaxation. This problem could be avoided by multi-step reverse electron transfer along the Trp-triad, e.g. [$FAD^{\bullet-}$ $TrpH_B$ $TrpH_C^{\bullet+}$] $\rightarrow$ [$FAD^{\bullet-}$ $TrpH_B^{\bullet+}$ $TrpH_C$] $\rightarrow$ FAD + $TrpH_B$ + $TrpH_C$, although it is not clear that this would be energetically feasible [58, 59]. Such electron hopping could be accompanied by strong J-modulation as discussed in section 3.

Turning now to the dipolar interaction, $|D(r)|$ only becomes comparable to the Zeeman interaction with the geomagnetic field (50 μT $\equiv$ 1.4 MHz) when $r = 3.8$ nm (equation (2)). In the x-ray structure of *At*Cry1 [28], the tryptophan and tyrosine residues that are furthest from the FAD are W447 at 2.90 nm and Y170 at 2.44 nm (edge-to-edge distances between aromatic rings). Neither is far enough away to have $|D(r)| < 1.4$ MHz and neither is part of an obvious electron transport chain linking it to the FAD. One way to realise a radical-radical separation exceeding 3.8 nm would be if the ultimate electron donor were located on another (unknown) protein complexed to the cryptochrome. Once again, a sequential reverse electron transfer pathway would be needed to allow fast enough singlet recombination. Finally, an effective radical separation as large as 3–4 nm could conceivably be contrived if the $FAD^{\bullet-}$ inside the cryptochrome were paired with a freely diffusing radical formed, for example, by electron transfer to the Trp radical in [$FAD^{\bullet-}$ $TrpH_C^{\bullet+}$]. Ascorbic acid has been discussed in this context [44].

In summary, although one can imagine cryptochrome-derived radical pair magnetic sensors in which J_{av} and D_{av} are small enough that they do not present a problem, such arrangements do not, at present, seem very likely.

5.3. Relaxation-enhanced compass sensitivity in cryptochrome

The results presented in figure 5 suggest that the anisotropic response of [$FAD^{\bullet -}$ $TrpH_C^{\bullet +}$] in *At*Cry 1 is particularly strongly enhanced for positive J_{av} in the range ~7 MHz to ~18 MHz. These values are of the same sign but somewhat larger than the only experimental measurements of this quantity (in different cryptochromes): 2.0 MHz [29] and 4.2 MHz [30]. However, it should be borne in mind that the exchange interaction depends on the separation of the radicals and the surrounding amino acid residues and could be larger in an avian magnetoreceptor cryptochrome than in a cryptochrome with a different biological function.

Although we have focussed here on the modulation of exchange and dipolar interactions, this is not the only source of spin relaxation. The other obvious contributors are (i) modulation of anisotropic hyperfine interactions by librational motions of the radicals within their binding sites and (ii) modulation of isotropic hyperfine interactions by conformational fluctuations, in particular in dihedral angles [47]. Further work will be needed to determine (a) whether the enhancements discussed here survive in the presence of these other spin-relaxation pathways and (b) the consequences of *J*-modulation and electron hopping occurring in tandem.

The simulations of [$FAD^{\bullet -}$ $TrpH_C^{\bullet +}$] described here were performed using a drastically simplified spin system, comprising two electron spins and two nuclear spins whose hyperfine tensors are those of the two ^{14}N nuclei (N5 and N10) in the central ring of the $FAD^{\bullet -}$ isoalloxazine ring system [44]. These two interactions—strongly axially anisotropic with parallel symmetry axes—dominate the spin dynamics of $FAD^{\bullet -}$ and arguably make flavin radicals near-optimal as components of a magnetic compass sensor [44, 60]. However, the influence of other nuclear spins cannot be discounted. In particular, a number of the hyperfine interactions in $TrpH_C^{\bullet +}$ are significantly anisotropic and of lower symmetry [44]. It seems likely that the lower the overall anisotropy of the radical pair, the less scope there would be for *J*-modulation to relax the spins anisotropically. Unfortunately it is difficult to explore this without much more efficient techniques for simulating large spin systems [61, 62]. Extending this line of argument, we speculate that the enhancement arising from *J*-modulation is more likely to be observed for a radical pair in which the $TrpH_C^{\bullet +}$ radical has been replaced by a radical with fewer, smaller, more isotropic hyperfine interactions (e.g. the ascorbyl radical [44]). Another reason in favour of a magnetically simpler partner for the $FAD^{\bullet -}$ radical is that any enhancement resulting from *J*-modulation would be less likely to be obscured by hyperfine-induced spin relaxation.

6. Conclusions

Previous work on radical pair magnetoreceptors has sought to identify, and in some cases quantify, the factors that control their sensitivity to the direction of the geomagnetic field. These properties include the identity of the radicals [44, 63, 64], their separation [25] and relative orientation [65], their hyperfine interactions [39, 44, 60, 66, 67], and their chemical kinetics [9, 67, 68]. Clearly, the molecular dynamics of the radicals must be added to this list given the profound effects electron spin relaxation can have on the spin-coherence. As argued here, modulation of spin interactions by molecular motions does not always simply degrade the performance of the sensor by destroying coherence. Under some circumstances, protein dynamics and appropriate magnetic interactions combine to produce anisotropic spin relaxation pathways that enhance the response of the compass to the direction of the geomagnetic field. Intermediate spin relaxation rates were found to be most effective. Evolution, acting through random mutations in the sequence of an avian cryptochrome, could have tuned not only its structural, magnetic and kinetic properties but also its dynamics for the purpose of magnetic sensing. In this regard, magnetoreception is no different from many other protein functions in which dynamics as well as structure play an essential role [69]. As in other areas of 'quantum biology' [70–72], interactions of the quantum system with a fluctuating environment appear to be critical for the quantum behaviour [58, 71]. An example, with a clear parallel to the present work, is 'environment assisted quantum transport' in which intermediate dephasing rates enhance the efficiency of photosynthetic energy transfer [73, 74].

Acknowledgments

We are grateful to Ye Jin and Jonathan Manouch for preliminary calculations. We thank the University of Oxford Advanced Research Computing (ARC) facility (http://dx.doi.org/10.5281/zenodo.22558) and the DeiC National HPC Center, University of Southern Denmark for generous allocation of CPU time. IAS is grateful for financial support from the Lundbeck Foundation and the Russian Science Foundation (Grant No.

14-12-00342). PJH thanks the European Research Council (under the European Union's 7th Framework Programme, FP7/2007-2013/ERC Grant Agreement No. 340451) and the Air Force Office of Scientific Research (Air Force Materiel Command, USAF Award No. FA9550-14-1-0095) for financial support.

Appendix A. Spin relaxation arising from *J*-modulation

Equation (7) and the STD term in equation (5) can be derived as follows. We start with the equation of motion of the radical pair density operator, $\hat{\rho}(t)$:

$$\frac{\mathrm{d}\hat{\rho}(t)}{\mathrm{d}t} = -\mathrm{i}[\hat{H}_0 + \hat{H}_\mathrm{I}(t),\, \hat{\rho}(t)] - k\hat{\rho}(t). \tag{11}$$

$\hat{H}_0$ is the time-independent part of the spin Hamiltonian containing the Zeeman and hyperfine interactions and the average exchange interaction. $k\,(=k_\mathrm{S}=k_\mathrm{T})$ is the rate constant for the formation of reaction products from the singlet and triplet states of the radical pair (figure 1(a)). $\hat{H}_\mathrm{I}(t)$ contains the time-dependence of the exchange interaction arising from fluctuations in the radical separation:

$$\hat{H}_\mathrm{I}(t) = F(t)\hat{h}_\mathrm{I}, \tag{12}$$

where

$$F(t) = J(r(t)) - J_\mathrm{av} = J(r(t)) - \langle J(r(t))\rangle, \tag{13}$$

$$\hat{h}_\mathrm{I} = -\left(2\hat{\mathbf{S}}_\mathrm{A}\cdot\hat{\mathbf{S}}_\mathrm{B} + \frac{1}{2}\hat{E}\right) = \hat{P}^\mathrm{S} - \hat{P}^\mathrm{T}, \tag{14}$$

$$\hat{P}^\mathrm{S} = \frac{1}{4}\hat{E} - \hat{\mathbf{S}}_A\cdot\hat{\mathbf{S}}_B \text{ and } \hat{P}^\mathrm{T} = \frac{3}{4}\hat{E} + \hat{\mathbf{S}}_\mathrm{A}\cdot\hat{\mathbf{S}}_\mathrm{B}. \tag{15}$$

$\hat{P}^\mathrm{S}$ and $\hat{P}^\mathrm{T}$ are the singlet and triplet projection operators, $\hat{E}$ is the identity operator, and $\hat{\mathbf{S}}_\mathrm{A}$ and $\hat{\mathbf{S}}_\mathrm{B}$ are the electron spin angular momentum operators of the two radicals. We assume that the correlation function for $J(r(t))$ decays exponentially with a correlation time τ_c,

$$\langle F(t)F(t+\tau)\rangle = \langle F(t)^2\rangle \exp(-\tau/\tau_\mathrm{c}) = \langle [J(r(t)) - J_\mathrm{av}]^2\rangle \exp(-\tau/\tau_\mathrm{c}) \tag{16}$$

and that the fluctuations in $F(t)$ are fast enough that

$$\langle [J(r(t)) - J_\mathrm{av}]^2\rangle \tau_\mathrm{c}^2 \ll 1. \tag{17}$$

Then, in the extreme narrowing limit, $\omega_{\alpha\beta}^2\tau_\mathrm{c}^2 \ll 1\ (\forall\ \alpha,\ \beta)$, where $\omega_{\alpha\beta}$ are $\hat{H}_0$ eigenvalue-differences, equation (11) becomes:

$$\frac{\mathrm{d}\hat{\rho}(t)}{\mathrm{d}t} + \mathrm{i}[\hat{H}_0,\, \hat{\rho}(t)] + k\hat{\rho}(t) = -\tau_\mathrm{c}\langle F(t)^2\rangle[\hat{h}_\mathrm{I},\, [\hat{h}_\mathrm{I},\, \hat{\rho}(t)]] = -k_\mathrm{STD}(\hat{P}^\mathrm{S}\hat{\rho}(t)\hat{P}^\mathrm{T} + \hat{P}^\mathrm{T}\hat{\rho}(t)\hat{P}^\mathrm{S}), \tag{18}$$

with k_STD given by equation (7). The operator part of equation (18) can be obtained using equations (14) and (19) and

$$(\hat{P}^\mathrm{S})^2 = \hat{P}^\mathrm{S};\quad (\hat{P}^\mathrm{T})^2 = \hat{P}^\mathrm{T};\quad \hat{P}^\mathrm{S}\hat{P}^\mathrm{T} = \hat{P}^\mathrm{T}\hat{P}^\mathrm{S} = 0;\quad \hat{P}^\mathrm{S} + \hat{P}^\mathrm{T} = \hat{E}. \tag{19}$$

We note that this approach could be extended to somewhat slower fluctuations, i.e. outside the extreme narrowing limit, using standard Redfield relaxation theory.

For the toy radical pair discussed in sections 2 and 3, the time-independent spin Hamiltonian is given by equation (6). More generally, for a radical pair with multiple, non-diagonal, rhombic hyperfine interactions, $\hat{H}_0$ has the form

$$\begin{aligned}\hat{H}_0 &= \hat{H}_{0\mathrm{A}} + \hat{H}_{0\mathrm{B}} - J_\mathrm{av}\left(2\hat{\mathbf{S}}_\mathrm{A}\cdot\hat{\mathbf{S}}_\mathrm{B} + \frac{1}{2}\hat{E}\right),\\ \hat{H}_{0K} &= \gamma_\mathrm{e}B_0[\hat{S}_{Kx}\sin\theta\cos\phi + \hat{S}_{Ky}\sin\theta\sin\phi + \hat{S}_{Kz}\cos\theta] + \sum_{j=1}^{N_K}[\hat{\mathbf{S}}_K\cdot\mathbf{A}_{Kj}\cdot\hat{\mathbf{I}}_{Kj}],\end{aligned} \tag{20}$$

where $K = \{\mathrm{A},\ \mathrm{B}\}$, and $\hat{\mathbf{I}}_{Kj}$ and $\mathbf{A}_{Kj}$ are the nuclear spin angular momentum operator and hyperfine tensor of nucleus j in radical K. N_K is the number of nuclear spins in radical K. Note that the spatial degrees of freedom are included in the spin Hamiltonian by means of effective parameters such as $\mathbf{A}_{Kj}$ and J_av.

A rough estimate of k_STD may be obtained by assuming a Gaussian distribution of separations, centred at $r = r_\mathrm{av}$, with standard deviation, σ:

$$f(r) = \frac{1}{\sqrt{2\pi}}\frac{1}{\sigma}\exp\left(-\frac{(r-r_\mathrm{av})^2}{2\sigma^2}\right). \tag{21}$$

Then, using equations (1) and (7):

$$k_{\mathrm{STD}} = 4\tau_{\mathrm{c}} \int_0^{\infty} f(r)[J(r(t)) - J_{\mathrm{av}}]^2 \mathrm{d}r = 4\tau_{\mathrm{c}} J_0^2 \exp(\beta^2\sigma^2) \exp(-2\beta r_{\mathrm{av}})(\exp[\beta^2\sigma^2] - 1). \tag{22}$$

When $J_0 = 8 \times 10^7$ T, $\beta = 14\ \mathrm{nm}^{-1}$, $r_{\mathrm{av}} = 1.9$ nm, $\sigma = 0.1$ nm, and $\tau_{\mathrm{c}} = 1$ ns, equation (22) gives $k_{\mathrm{STD}} = 2.7 \times 10^8\ \mathrm{s}^{-1}$.

Appendix B. Spin relaxation arising from *D*-modulation

The relaxation arising from fluctuations in the dipolar interaction may be treated in the same way as *J*-modulation. The analogous expressions to equations (13) and (14) are:

$$F(t) = D(r(t)) - D_{\mathrm{av}} = D(r(t)) - \langle D(r(t))\rangle, \tag{23}$$

$$\hat{h}_1 = \frac{2}{3}(3\hat{S}_{\mathrm{Az}}\hat{S}_{\mathrm{Bz}} - \hat{\boldsymbol{S}}_{\mathrm{A}} \cdot \hat{\boldsymbol{S}}_{\mathrm{B}}) = \frac{1}{3}\hat{P}^{\mathrm{T}_+} + \frac{1}{3}\hat{P}^{\mathrm{T}_-} - \frac{2}{3}\hat{P}^{\mathrm{T}_0}, \tag{24}$$

where $\hat{P}^{\mathrm{T}_m}$ is the projection operator for the T_m triplet state ($m = 0, \pm 1$). The evolution of the density operator is:

$$\begin{aligned}\frac{\mathrm{d}\hat{\rho}(t)}{\mathrm{d}t} &+ \mathrm{i}[\hat{H}_0, \hat{\rho}(t)] + k\hat{\rho}(t) = -\tau_{\mathrm{c}}\langle F(t)^2\rangle[\hat{h}_1, [\hat{h}_1, \hat{\rho}(t)]] \\ &= -\tau_{\mathrm{c}}\langle[D(r(t)) - D_{\mathrm{av}}]^2\rangle\Big[\frac{1}{9}\hat{P}^{\mathrm{S}}\hat{\rho}(t)\hat{P}^{\mathrm{T}_+} + \frac{1}{9}\hat{P}^{\mathrm{T}_+}\hat{\rho}(t)\hat{P}^{\mathrm{S}} + \frac{1}{9}\hat{P}^{\mathrm{S}}\hat{\rho}(t)\hat{P}^{\mathrm{T}_-} + \frac{1}{9}\hat{P}^{\mathrm{T}_-}\hat{\rho}(t)\hat{P}^{\mathrm{S}} \\ &\quad + \frac{4}{9}\hat{P}^{\mathrm{S}}\hat{\rho}(t)\hat{P}^{\mathrm{T}_0} + \frac{4}{9}\hat{P}^{\mathrm{T}_0}\hat{\rho}(t)\hat{P}^{\mathrm{S}} + \hat{P}^{\mathrm{T}_+}\hat{\rho}(t)\hat{P}^{\mathrm{T}_0} + \hat{P}^{\mathrm{T}_0}\hat{\rho}(t)\hat{P}^{\mathrm{T}_+} \\ &\quad + \hat{P}^{\mathrm{T}_-}\hat{\rho}(t)\hat{P}^{\mathrm{T}_0} + \hat{P}^{\mathrm{T}_0}\hat{\rho}(t)\hat{P}^{\mathrm{T}_-}\Big].\end{aligned} \tag{25}$$

It can be seen from equation (25) that *D*-modulation leads not only to STD but also to triplet–triplet dephasing; density matrix elements such as $\langle \mathrm{T}_{+1}|\ \hat{\rho}(t)|\mathrm{T}_0\rangle$ and $\langle \mathrm{T}_{-1}|\ \hat{\rho}(t)|\mathrm{T}_0\rangle$ (but not $\langle \mathrm{T}_{+1}|\ \hat{\rho}(t)|\mathrm{T}_{-1}\rangle$) are relaxed. $\hat{H}_0$ in equation (25) is given by equations (6) or (20) with the exchange term replaced by $\frac{2}{3}D_{\mathrm{av}}(3\hat{S}_{\mathrm{Az}}\hat{S}_{\mathrm{Bz}} - \hat{\boldsymbol{S}}_{\mathrm{A}} \cdot \hat{\boldsymbol{S}}_{\mathrm{B}})$.

Using $r_{\mathrm{av}} = 1.9$ nm, $\sigma = 0.1$ nm, and $\tau_{\mathrm{c}} = 1$ ns (as above, equation (21)), the dipolar relaxation rate constant is:

$$k_{\mathrm{D}} = \tau_{\mathrm{c}}\langle[D(r(t)) - D_{\mathrm{av}}]^2\rangle = \tau_{\mathrm{c}}\int_0^{\infty} f(r)[D(r(t)) - D_{\mathrm{av}}]^2 \mathrm{d}r = 1.4 \times 10^5\ \mathrm{s}^{-1}. \tag{26}$$

This value is substantially smaller than the corresponding estimate of k_{STD} for *J*-modulation ($2.7 \times 10^8\ \mathrm{s}^{-1}$) because the dipolar interaction has a much weaker dependence on *r*.

Appendix C. Spin relaxation arising from the random fields mechanism

A corresponding treatment of the 'random fields' relaxation mechanism proceeds as follows. The time-dependent part of the spin Hamiltonian is

$$\hat{H}_1(t) = \sum_K \sum_j F_{Kj}(t)\hat{S}_{Kj}, \tag{27}$$

with

$$\langle F_{Kj}(t)\rangle = 0 \text{ and } \langle F_{Kj}(t)F_{K'j'}(t+\tau)\rangle = \delta_{KK'}\delta_{jj'}\langle F(t)^2\rangle \exp(-\tau/\tau_{\mathrm{R}}),$$

where $\hat{S}_{Kj}$ is the *j*-component ($j = x, y, z$) of the electron spin operator for radical *K* ($K = \mathrm{A}, \mathrm{B}$). Hence:

$$\begin{aligned}\frac{\mathrm{d}\hat{\rho}(t)}{\mathrm{d}t} + \mathrm{i}[\hat{H}_0, \hat{\rho}(t)] + k\hat{\rho}(t) &= -\tau_{\mathrm{R}}\langle F(t)^2\rangle \sum_K \sum_j \Big[\hat{S}_{Kj}, [\hat{S}_{Kj}, \hat{\rho}(t)]\Big] \\ &= -k_{\mathrm{RFR}}\Big\{\frac{3}{2}\hat{\rho}(t) - \sum_K \sum_j \hat{S}_{Kj}\hat{\rho}(t)\hat{S}_{Kj}\Big\},\end{aligned} \tag{29}$$

with

$$k_{\mathrm{RFR}} = 2\tau_{\mathrm{R}}\langle F(t)^2\rangle. \tag{30}$$

Appendix D. Spin relaxation arising from electron hopping

The effects of the J-modulation caused by electron hopping between RP_0 and RP_1 (figure 1(c)) were modelled by means of coupled Liouville equations for the two density operators:

$$\begin{aligned}\frac{d\sigma_0(t)}{dt} &= -L_0\sigma_0(t) + k_{10}\sigma_1(t) - k_{01}\sigma_0(t),\\ \frac{d\sigma_1(t)}{dt} &= -L_1\sigma_1(t) - k_{10}\sigma_1(t) + k_{01}\sigma_0(t),\end{aligned} \tag{31}$$

in which k_{10} and k_{01} are the first order rate constants for $RP_1 \rightarrow RP_0$ and $RP_0 \rightarrow RP_1$ respectively and $\sigma_0(t)$ and $\sigma_1(t)$ are the vector representations of the two density operators, $\hat{\rho}_0(t)$ and $\hat{\rho}_1(t)$. The matrix representations of the two Liouvillian superoperators are

$$\begin{aligned}L_0 &= \mathrm{i}\left(\hat{H}_0^{(0)} \otimes \hat{E} - \hat{E} \otimes \hat{H}_0^{(0)\mathrm{T}}\right),\\ L_1 &= \mathrm{i}\left(\hat{H}_0^{(1)} \otimes \hat{E} - \hat{E} \otimes \hat{H}_0^{(1)\mathrm{T}}\right) + \frac{k_\mathrm{b}}{2}\left(\hat{P}^\mathrm{S} \otimes \hat{E} + \hat{E} \otimes \hat{P}^\mathrm{S}\right) + k_\mathrm{f}\hat{E} \otimes \hat{E}.\end{aligned} \tag{32}$$

The rate constants k_b and k_f are defined in figure 1(c). Superscript T denotes transpose. The two spin Hamiltonians are

$$\begin{aligned}\hat{H}_0^{(0)} &= -J_{\mathrm{RP0}}\left(2\hat{\mathbf{S}}_\mathrm{A}\cdot\hat{\mathbf{S}}_\mathrm{B} + \frac{1}{2}\hat{E}\right),\\ \hat{H}_0^{(1)} &= -J_{\mathrm{RP1}}\left(2\hat{\mathbf{S}}_\mathrm{A}\cdot\hat{\mathbf{S}}_\mathrm{B} + \frac{1}{2}\hat{E}\right) + \hat{H}_\mathrm{Z}^{(1)} + \hat{H}_\mathrm{HFC}^{(1)}.\end{aligned} \tag{33}$$

$\hat{H}_\mathrm{Z}^{(1)}$ and $\hat{H}_\mathrm{HFC}^{(1)}$ are the Zeeman and hyperfine interactions in RP_1 (see equation (6)). It was assumed that J_{RP_0}, the exchange interaction in RP_0, is so large that the Zeeman and hyperfine interactions in RP_0 have a negligible effect on its spin dynamics. The singlet product yield was calculated by assembling a joint Liouville space for the two sites:

$$\frac{\mathrm{d}}{\mathrm{d}t}\begin{pmatrix}\sigma_0(t)\\ \sigma_1(t)\end{pmatrix} = -\begin{pmatrix}L_0 + k_{01}E & -k_{10}E\\ -k_{01}E & L_1 + k_{10}E\end{pmatrix}\begin{pmatrix}\sigma_0(t)\\ \sigma_1(t)\end{pmatrix} = -\mathbf{\Lambda}\begin{pmatrix}\sigma_0(t)\\ \sigma_1(t)\end{pmatrix} \tag{34}$$

so that

$$\begin{pmatrix}\sigma_0(t)\\ \sigma_1(t)\end{pmatrix} = \exp(-\mathbf{\Lambda}t)\begin{pmatrix}\sigma_0(0)\\ \sigma_1(0)\end{pmatrix}. \tag{35}$$

The singlet yield is then

$$\begin{aligned}\Phi_\mathrm{S} &= k_\mathrm{b}\int_0^\infty \mathrm{Tr}[P^\mathrm{S}\sigma_1(t)]\,\mathrm{d}t\\ &= k_\mathrm{b}\int_0^\infty (0 \quad P^\mathrm{S})\exp(-\mathbf{\Lambda}t)\begin{pmatrix}\sigma_0(0)\\ \sigma_1(0)\end{pmatrix}\mathrm{d}t\\ &= \frac{k_\mathrm{b}}{Z}(0 \quad P^\mathrm{S})\mathbf{\Lambda}^{-1}\begin{pmatrix}P^\mathrm{S}\\ 0\end{pmatrix}\end{aligned} \tag{36}$$

using the initial condition $\sigma_0(0) = P^\mathrm{S}/Z$ where Z is the total number of nuclear spin configurations.

References

[1] Steiner U E and Ulrich T 1989 *Chem. Rev.* **89** 51
[2] Rodgers C T 2009 *Pure Appl. Chem.* **81** 19
[3] Schulten K, Swenberg CE and Weller A 1978 *Z. Phys. Chem. NF* **111** 1
[4] Wiltschko W 1968 *Z. Tierpsychol.* **25** 537
[5] Wiltschko W and Wiltschko R 1972 *Science* **176** 62
[6] Wiltschko R and Wiltschko W 1995 *Magnetic Orientation in Animals* (Berlin: Springer)
[7] Mouritsen H 2014 *Sturkie's Avian Physiology* ed C Scanes (New York: Elsevier) p 113
[8] Ritz T, Adem S and Schulten K 2000 *Biophys. J.* **78** 707
[9] Rodgers C T and Hore P J 2009 *Proc. Natl Acad. Sci. USA* **106** 353
[10] Phillips J B, Jorge P E and Muheim R 2010 *J. R. Soc. Interface* **7** S241
[11] Ritz T, Ahmad M, Mouritsen H, Wiltschko R and Wiltschko W 2010 *J. R. Soc. Interface* **7** S135
[12] Liedvogel M and Mouritsen H 2010 *J. R. Soc. Interface* **7** S147
[13] Ritz T 2011 *Proc. Chem.* **3** 262
[14] Dodson C A, Hore P J and Wallace M I 2013 *Trends Biochem. Sci.* **38** 435
[15] Solov'yov I A, Ritz T, Schulten K and Hore P J 2014 *Quantum Effects in Biology* ed M Mohseni *et al* (Cambridge: Cambridge University Press) p 218

[16] Holland RA 2014 *J. Zool.* **293** 1
[17] Hore PJ and Mouritsen H 2016 *Ann. Rev. Biophys.* **45** 299
[18] Gindt Y M, Vollenbroek E, Westphal K, Sackett H, Sancar A and Babcock G T 1999 *Biochemistry* **38** 3857
[19] Giovani B, Byrdin M, Ahmad M and Brettel K 2003 *Nat. Struct. Biol.* **10** 489
[20] Zeugner A *et al* 2005 *J. Biol. Chem.* **280** 19437
[21] Biskup T *et al* 2009 *Angew. Chem., Int. Ed. Engl.* **48** 404
[22] Henbest K B *et al* 2008 *Proc. Natl Acad. Sci. USA* **105** 14395
[23] Maeda K *et al* 2012 *Proc. Natl Acad. Sci. USA* **109** 4774
[24] Atherton N M 1993 *Principles of Electron Spin Resonance* (Chichester: Ellis Horwood)
[25] Efimova O and Hore P J 2008 *Biophys. J.* **94** 1565
[26] O'Dea A R, Curtis A F, Green N J B, Timmel C R and Hore P J 2005 *J. Phys. Chem.* A **109** 869
[27] Moser C C, Keske J M, Warncke K, Farid R S and Dutton P L 1992 *Nature* **355** 796
[28] Brautigam C A *et al* 2004 *Proc. Natl Acad. Sci. USA* **101** 12142
[29] Biskup T *et al* 2011 *Angew. Chem,. Int. Ed. Engl.* **50** 12647
[30] Weber S *et al* 2010 *J. Phys. Chem.* B **114** 14745
[31] Hulsebosch R J, Borovykh I V, Paschenko S V, Gast P and Hoff A J 1999 *J. Phys. Chem.* B **103** 6815
[32] Proskuryakov I I, Klenina I B, Hore P J, Bosch M K, Gast P and Hoff A J 1996 *Chem. Phys. Lett.* **257** 333
[33] Till U, Klenina I B, Proskuryakov I I, Hoff A J and Hore P J 1997 *J. Phys. Chem.* B **101** 10939
[34] Dellis A T and Kominis I K 2012 *BioSyst.* **107** 153
[35] Lau J C S, Wagner-Rundell N, Rodgers C T, Green N J B and Hore P J 2010 *J. R. Soc. Interface* **7** S257
[36] Gauger E M, Rieper E, Morton J J L, Benjamin S C and Vedral V 2011 *Phys. Rev. Lett.* **106** 040503
[37] Cai J, Caruso F and Plenio M B 2012 *Phys. Rev.* A **85** 040304
[38] Bandyopadhyay J N, Paterek T and Kaszlikowski D 2012 *Phys. Rev. Lett.* **109** 110502
[39] Cai J M and Plenio M B 2013 *Phys. Rev. Lett.* **111** 230503
[40] Gauger E M and Benjamin S C 2013 *Phys. Rev. Lett.* **110** 178901
[41] Xu B M, Zou J, Li H, Li J G and Shao B 2014 *Phys. Rev.* E **90** 042711
[42] Walters Z B 2014 *Phys. Rev.* E **90** 042710
[43] Carrillo A, Cornelio M F and de Oliveira M C 2015 *Phys. Rev.* E **92** 012720
[44] Lee A A, Lau J C S, Hogben H J, Biskup T, Kattnig D R and Hore P J 2014 *J. R. Soc. Interface* **11** 20131063
[45] Shushin A I 1991 *Chem. Phys. Lett.* **181** 274
[46] Nielsen M A and Chuang I L 2010 *Quantum Computation and Quantum Information* (New York: Cambridge University Press)
[47] Kattnig D R, Solov'yov I A and Hore P J 2016 *Phys. Chem. Chem. Phys.* **18** 12443
[48] Solov'yov I A, Domratcheva T, Shahi A R M and Schulten K 2012 *J. Am. Chem. Soc.* **134** 18046
[49] Solov'yov I A, Yakubovich A V, Nikolaev P V, Volkovets I and Solov'yov A V 2012 *J. Comput. Chem.* **33** 2412
[50] Phillips J C *et al* 2005 *J. Comput. Chem.* **26** 1781
[51] Gamliel D and Levanon H 1995 *Stochastic Processes in Magnetic Resonance* (Singapore: World Scientific)
[52] Breuer H-P and Petruccione F 2002 *The Theory of Open Quantum Systems* (New York: Oxford University Press)
[53] Kattnig D R *et al* 2016 *Nat. Chem.* **8** 384
[54] Engelhard C *et al* 2014 *Plant Cell* **26** 4519
[55] El-Esawi M, Glascoe A, Engle D, Ritz T, Link J and Ahmad M 2015 *Plant Signal. Behav.* **10** e1063758
[56] Müller P, Yamamoto J, Martin R, Iwai S and Brettel K 2015 *Chem. Commun.* **51** 15502
[57] Cailliez F, Müller P, Firmino T, Pernot P and de la Lande A 2016 *J. Am. Chem. Soc.* **138** 1904
[58] Lüdemann G, Solov'yov I A, Kubar T and Elstner M 2015 *J. Am. Chem. Soc.* **137** 1147
[59] Sjulstok E, Olsen J M H and Solov'yov I A 2015 *Sci. Rep.* **5** 18446
[60] Cintolesi F, Ritz T, Kay C W M, Timmel C R and Hore P J 2003 *Chem. Phys.* **294** 385
[61] Manolopoulos D E and Hore P J 2013 *J. Chem. Phys.* **139** 124106
[62] Lewis A M, Manolopoulos D E and Hore P J 2014 *J. Chem. Phys.* **141** 044111
[63] Hogben H J, Efimova O, Wagner-Rundell N, Timmel C R and Hore P J 2009 *Chem. Phys. Lett.* **480** 118
[64] Solov'yov I A and Schulten K 2009 *Biophys. J.* **96** 4804
[65] Rodgers C T 2007 Magnetic field effects in chemical systems *D. Phil. Thesis* University of Oxford
[66] Lambert N, De Liberato S, Emary C and Nori F 2013 *New J. Phys.* **15** 083024
[67] Hiscock H G *et al* 2016 *Proc. Natl Acad. Sci. USA* **113** 4634
[68] Solov'yov I A, Chandler D E and Schulten K 2007 *Biophys. J.* **92** 2711
[69] Mittermaier A and Kay L E 2006 *Science* **312** 224
[70] Al-Khalili J and McFadden J 2014 *Life on The Edge: The Coming of Age of Quantum Biology* (London: Bantam)
[71] Huelga S F and Plenio M B 2013 *Contemp. Phys.* **54** 181
[72] Lambert N, Chen Y N, Cheng Y C, Li C M, Chen G Y and Nori F 2013 *Nat. Phys.* **9** 10
[73] Rebentrost P, Mohseni M, Kassal I, Lloyd S and Aspuru-Guzik A 2009 *New J. Phys.* **11** 033003
[74] Mohseni M, Rebentrost P, Lloyd S and Aspuru-Guzik A 2008 *J. Chem. Phys.* **129** 174106